

Coregistration of QuickBird Imagery and Digital Map Using a Modified ICP Algorithm

수정된 ICP알고리즘을 이용한 수치지도와 QuickBird 영상의 보정

Dongyeob Han¹⁾ · Yangdam Eo²⁾ · Yonghyun Kim³⁾ · Kwangjae Lee⁴⁾ · Younsoo Kim⁵⁾
한동엽 · 어양담 · 김용현 · 이광재 · 김윤수

Abstract

For geometric correction of high-resolution images, the authors matched corresponding objects between a large-scale digital map and a QuickBird image to obtain the coefficients of the first order polynomial. Proximity corrections were performed, using the Boolean operation, to perform automated matching accurately. The modified iterative closest point (ICP) algorithm was used between the point data of the surface linear objects and the point data of the edge objects of the image to determine accurate transformation coefficients. As a result of the automated geometric correction for the study site, an accuracy of 1.207 root mean square error (RMSE) per pixel was obtained.

Keywords : Coregistration, RPC, proximity correction, ICP

1. Introduction

Since the spatial resolution of satellite images has rapidly improved, the images have played an important role in map updating and geographic information system (GIS) data gathering. When satellite images are provided to GIS users, they should be registered by geo-coordinates. However, such a process is costly and time consuming, since it includes a spot survey for ground control point (GCP) collection. A number of research projects are investigating the quick and accurate registration of images to develop cost-effective registration solutions(Wang etc., 2008; Gianinetta etc., 2008; Wong etc., 2007; Eugenio etc., 2003).

We propose a method for the automatic registration of

satellite images using a digital map. By using an existing digital map, cost saving is an additional benefit. In this paper, a two-step registration process is proposed, in which the first step involves determining proximity transformation relationships. The second step involves performing a precise least square adjustment using a modified iterative closest point (ICP) algorithm. The flow of research is shown in Figure 1.

For selecting corresponding objects within both the digital map and the satellite image, the modified ICP algorithm is tested. ICP is the method used to find the transformation function by locating matching pairs between the model and scene data under the condition of minimum distance. There has been much improvement in the method of enhancing convergence speed and the method of determining and calculating

1) Regular member · Assistant professor, Department of Civil and Environmental Engineering, Chonnam National University (E-mail:hozilla @chonnam.ac.kr)

2) Regular member · Corresponding author, Assistant professor, Department of Advanced Fusion Technology, Konkuk University (E-mail:coandrew@konkuk.ac.kr)

3) Regular member · Satellite Data Application Department, Satellite Information Research Institute, KARI (E-mail: kyh@kari.re.kr)

4) Regular member · Satellite Data Application Department, Satellite Information Research Institute, KARI (E-mail:kjlee@kari.re.kr)

5) Regular member · Satellite Data Application Department, Satellite Information Research Institute, KARI (E-mail:younsoo@kari.re.kr)

error metrics for exact matching, since the methodic introductions of various researchers(Chen etc.,1991; Besl etc., 1992; Rusinkiewicz etc., 2001).

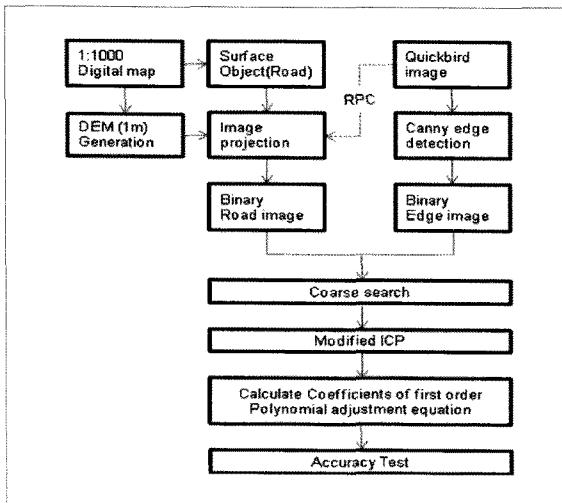


Fig. 1. Flow of research.

2. Proposed Method

Common methods used to register a high-resolution satellite image geometrically are the rigorous sensor model that uses the supplied attitude and ephemeris files or rational polynomial coefficients (RPCs), which offer mathematical mapping from object-space coordinates to image coordinates(Aguilar etc., 2007; Habib etc., 2007). The registration process by RPCs is comparatively simple, and its orthorectification accuracies are 3–6 m of root mean square error (RMSE) in the case of a QuickBird satellite image. To improve the accuracy of registration by RPCs, a few GCPs may be manually added in the registration process. This registration method uses corresponding objects in place of GCPs. Such corresponding objects are selected from archived digital maps with the same spatial extent as the high-resolution images. To determine the degree of correspondence amongst the corresponding surface objects, binarized feature elements from the two sets of data are generated and searched. We can then estimate each resolution error of the image by using both rotation and translation transformations as proposed by Grodecki and Dial (2003), which was validated by space imaging:

$$\Delta P = A_0 + AS \cdot Col + AL \cdot Line + ASL \cdot Col \cdot Line + \dots \quad (1)$$

$$\Delta R = B_0 + BS \cdot Col + BL \cdot Line + BSL \cdot Col \cdot Line + \dots$$

Where: Col, Line represents column and row of the image.

A_0, AS, AL, B_0, BS, E are adjustment coefficients.

ΔP are adjustment errors of the column and row.

Since the errors are distributed in such simple forms, appropriate transformation coefficients can be approximately estimated by designating the surface objects as a control image and moving the satellite image onto them. Since the surface objects of the digital map are vector data, their plane locations are located on each node. We can obtain 3D information by reading the height information of each node location from the DEM. Binary images of the surface objects can be generated by rasterizing each segment of the objects into the size of the image pixels, after transforming the 3D surface object data into satellite image spaces by using RPC.

Objects considered surface objects are searched by edge extraction from the satellite images. In addition, binary images are generated from the edges. In the case where the two binary image values at the same location in the image space are 1, the location points are considered possible corresponding points. It is also possible to adjust the overall movement range and the movement cell size in various ways for the purpose of reducing the number of operations. Proximity adjustment is carried out for every five pixels in the direction of line columns, while a precise adjustment is performed for every single pixel. Figure 2 shows an overlay of the digital binary image and the edge image after proximity adjustment.

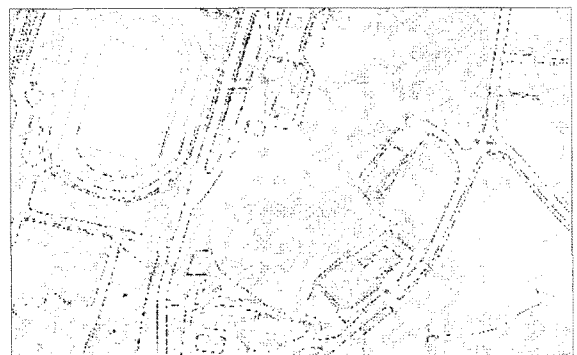


Fig. 2. Overlay of the binarized digital map (red) and the binarized edge of the satellite image (cyan) after proximity adjustment.

The ICP algorithm mainly uses a 3D coordinate system, which is geometrical, using plane locations and height differences. The ICP algorithm also uses colors, surface orientation and invariant and other features instead of, or together with, heights (Silva etc., 2005; Yamany etc., 1999; Sharp etc., 2002). The brightness values of a satellite image do not have a strong relationship with the height values in digital maps, which utilize point data of the azimuth angle composed of X, Y and A (azimuth) as input data, instead of X, Y and Z. The average minimum distance between the point data of the azimuth angle was used as the error function. When two corresponding point sets $\{m_i\}$ and $\{s_i\}$, and $i = 1, \dots, N$ exist, and they are interconnected similarly to Formula (1) shown below, the theory of least square error is applied to obtain the optimal transformation formula $[\hat{R}, \hat{T}]$ that performs correction so that set $\{m_i\}$ can be properly overlaid with set $\{s_i\}$.

$$s_i = Rm_i + T + v_i \tag{2}$$

$$\sum_{i=1}^N v_i^2 = \sum_{i=1}^N \|s_i - \hat{R}m_i - \hat{T}\|^2 \tag{3}$$

If outliers exist in the corresponding pairs, the least square method cannot obtain the optimal solution. Therefore, the solution should be obtained using another method. When we try to obtain the solution using singular value decomposition (SVD), the two point sets $\{m_i\}$ and $\{s_i\}$ should have the same center as a result of the least square solution of Formula (2). Using this constraint condition, we can obtain the rotation matrices \hat{R} and \hat{T} .

Figure 3 shows the process of changing the input data into the point data of the azimuth angle and then applying them to the ICP algorithm designed to obtain the solution. The azimuth angle of individual objects should be extracted from the digital map and the image to generate the point data of the azimuth angle. In the digital terrain map, polylines are composed of segments. In grid data, such as images or digital height models, those parts in which data properties significantly change can be extracted as edges. The extracted edges can then be distinguished and sorted into several segments through connected component labeling. When there are endpoints of a segment $A(x_1, y_1)$, $B(x_2, y_2)$ in a 2D plane, the sampling formula of \overline{AB} is as follows (refer to Figure 4).

When transforming P, a point datum of the azimuth angle, according to Q point data, initialize $P_0 = P$ and rotation matrix $R_0 = 1$. Estimate T_0 , the initial value of the translation matrix, by evaluating the similarity.

For $K = 0$: number of the maximum repetition.

*Find the minimum distance matching pair between P_k and Q in Euclidean distance.

*Obtain R_k , a rotation matrix, and T_k , a translation matrix, that minimize the errors between the matching pair.

*Apply the transformation formula to $P_k P_{k+2} = R_k(P_k) + T_k$.

*When the average square errors are smaller than the critical value, stop the repetition.

Fig. 3. ICP pseudocode for the registration between the point data of the azimuth angle.

$$\text{Sampled Points } (i) = i \times \bar{n} + A \tag{4}$$

Where, $m = \text{floor}\left(\frac{\text{Distance}(A,B)}{\text{SampleResolution}}\right)$ (5)

$$\bar{n} = \frac{(B-A)}{m} \tag{6}$$

$$i = 1, \dots, m \tag{7}$$

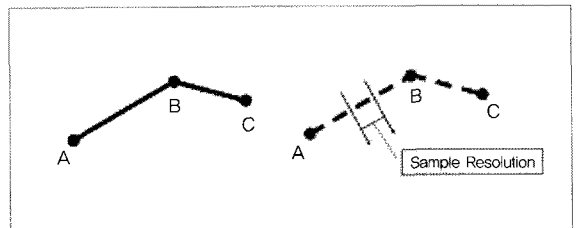


Fig. 4. Points sampling from a polyline object.

When the endpoints of a segment are $A(x_1, y_1)$, $B(x_2, y_2)$ in 2D plane data, the azimuth angle of the segment (A) can be obtained through the formula shown below.

$$A = \tan^{-1}\left(\frac{x_1 - x_2}{y_1 - y_2}\right) \tag{8}$$

3. Experiment and Analysis

A QuickBird panchromatic image was used for the experiment. Table 1 shows the image specifications. Part of Daejeon, Korea, was selected as the study site. The study area is 6 × 6 km and includes forest and rivers, as well as the downtown urban area. The elevation data was interpolated with a spatial resolution of 1 m, after the height point layers and the contour layers of the digital map were TIN-transformed using ESRI ArcGIS. The range of the height value was 31.87–190.59 m. After polyline rasterization with 0.5 m interval was performed, the heights of the road objects on the digital map from the digital terrain model (DTM) were obtained for the QuickBird image.

Table 1. Specifications of QuickBird image.

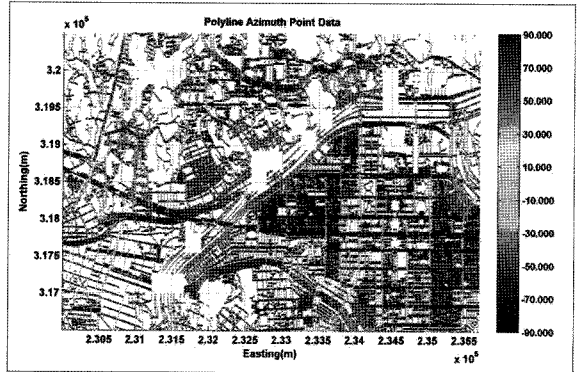
Product Level	Row GSD	Column GSD	Mean Sun Azimuth	Mean Sun Elevation	Mean Sat. Azimuth	Mean Sat. Elevation	DEM Correction
LV2A	0.800 m	0.723 m	160.5°	30.2°	199.3°	59.4°	Base Elevation



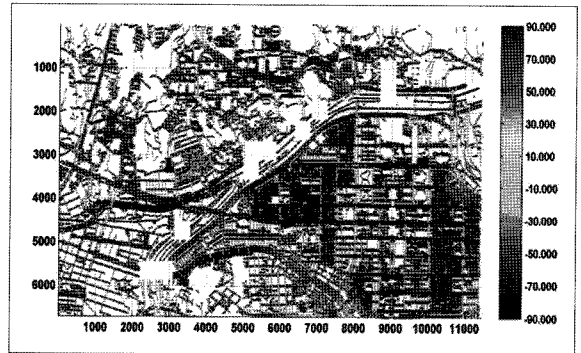
Fig. 5. QuickBird image used for research.

The binary control object data from the road layer and the binary edge point data from the image (refer to Figure 6). Because the binary control object data, which has an eastward/northward value, was projected onto the QuickBird

image, the points from each data have row, column and azimuth values. The azimuth value was -90 to +90 degrees. The Canny edge detector was used for detection of the binary edges from the QuickBird image. After identifying all edges through using connected component labeling, small-sized edges with a maximum of 40 points were deleted for computational efficiency.



(a) image edge



(b) surface object

Fig. 6. Point data of the azimuth angle.

To determine the initial transformation factors relatively accurately, we designated the range of factors and the appropriate size of cells and searched for the point of maximum similarity between the data within the range. The optimal locations in the section -70 to +70 pixels are the column and row displacements 59–22, respectively. The QuickBird binary edge point data was offset by a coarse registration result. The correction polynomial coefficients were estimated by performing the modified ICP using the point data with X, Y and A.

After transformation, for each transformed point in the

QuickBird point data, the closest point in the control object point data was determined. In this experiment, the threshold for the number of iterations was set at 30, and the threshold for the change of distance sum was set at 0.0001 m. These values were determined empirically. The detected matching points are distributed evenly within the study area (refer to Figure 7). After the eighth iteration, a total of 55,861 points were selected for the linear correction. Table 2 shows the final coefficients of the first-order polynomial transformation.

For accuracy comparison with the proposed method, 37 ground points with a regular geometric distribution over the entire study area were selected as independent check points for evaluating the geo-rectification accuracy.



Fig. 7. Corresponding points used for fine coregistration.

Table 2. Estimated parameters for the first-order polynomial transformation.

parameters	ΔP			ΔR		
	A_0	AS	AL	B_0	BS	BL
values	58.85	1.0000 08	-0.000 019	-23.06	0.0000 38	1.000 150

As a result, there are 0.941 pixels RMSE, 0.755 pixels RMSE and 1.207 pixels overall RMSE at 37 independent check points.

4. Conclusion

From the results of the experiment it was reasoned that, as sensor performances have continuously improved, research activities will become more and more active in the area of

improving accuracies using various terrain data. Also, a variety of future studies based on the existing accumulated data will be conducted. In this study, the authors corrected the QuickBird image using an automated method, utilizing the surface objects and the height information from the large-scale digital terrain map. As a result of the correction performed for the study site, an accuracy of 1.207 pixels RMSE was obtained. The authors are planning to conduct future research on how to directly renew RPC and develop a method to obtain automatically the 3D information of objects from 3D high-resolution images.

Acknowledgement

This work was supported by the Korea Aerospace Research Institute through a grant from the KOMPSAT-3 system development project.

References

- Aguilar, M.A., Aguilar, F.J., Agüera, F. and Sánchez, J.A. (2007), Geometric accuracy assessment of QuickBird basic imagery using different operational approaches, *Photogrammetric Engineering and Remote Sensing*, Vol. 73, No. 12, pp. 1321-1332.
- Besl, P. and McKay, N. (1992), A method for registration of 3-D shapes, *IEEE Transaction on Pattern Analysis and Machine Intelligence*, Vol. 14, No. 2, pp. 239-256.
- Chen, Y. and Medioni, G. (1991), Object modeling by registration of multiple range images, *IEEE International Conference on Robotics and Automation*.
- Eugenio, F. and Marques, F. (2003), Automatic satellite image georeferencing using a contour-matching approach, *IEEE Transactions on Geoscience and Remote Sensing*, Vol. 41, No. 12, pp. 2869-2880.
- Gianinetto, M. and Scaioni, M. (2008), Automated geometric correction of high-resolution pushbroom satellite data, *Photogrammetric Engineering and Remote Sensing*, Vol. 74, No. 1, pp. 107-116.
- Habib, A., Kim, K., Shin, S.W., Kim, C., Bang, K.I., Kim, E.M. and Lee, D.C. (2007), Comprehensive analysis of

- sensor modeling alternatives for high-resolution imaging satellites, *Photogrammetric Engineering and Remote Sensing*, Vol. 73, No. 11, pp. 1241-1252.
- Rusinkiewicz, S. and Levoy, M. (2001), Efficient variants of the ICP algorithm, *Third International Conference on 3-D Digital Imaging and Modeling*, pp. 145-152.
- Sharp, G.C., Lee, S.W. and Wehe, D.K. (2002), ICP registration using invariant features, *IEEE Transaction on Pattern Analysis and Machine Intelligence*, Vol. 24, No. 1, pp. 90-102.
- Silva, L., Bellon, O. and Boyer, K.L. (2005), Precision range image registration using a robust surface interpenetration measure and enhanced genetic algorithms, *IEEE Transaction on Pattern Analysis and Machine Intelligence*, Vol. 27, No. 5, pp. 762-776.
- Wang, C.X., Stefanidis, A., Croitoru, A. and Agouris, P. (2008), Map registration of image sequences using linear features, *Photogrammetric Engineering and Remote Sensing*, Vol. 74, No. 1, pp. 25-38.
- Wong, A. and Clausi, D.A. (2007), ARRSI: Automatic registration of remote-sensing Images, *IEEE Transactions on Geoscience and Remote Sensing*, Vol. 45, No. 5, pp. 1483-1493.
- Yamany, S. and Farag, A. (1999), Free-form surface registration using surface signatures, *Proceedings of Int'l Conf. Computer Vision*, pp. 1098-1104.

(접수일 2010. 12. 06, 심사일 2010. 12. 10, 심사완료일 2010. 12. 10)